

# Drivers of soil organic carbon from temperate to alpine forests: a model-based analysis of the Swiss forest soil inventory with Yasso20

Claudia Guidi<sup>1\*</sup>, Sia Gosheva-Oney<sup>1,2\*</sup>, Markus Didion<sup>1</sup>, Roman Flury<sup>1</sup>, Lorenz Walthert<sup>1</sup>, Stephan Zimmermann<sup>1</sup>, Brian J. Oney<sup>1</sup>, Pascal A. Niklaus<sup>2</sup>, Esther Thürig<sup>1</sup>, Toni Viskari<sup>3,4</sup>, Jari Liski<sup>3</sup>, Frank Hagedorn<sup>1</sup>

<sup>1</sup>Swiss Federal Institute for Forest, Snow and Landscape Research WSL, Birmensdorf, Switzerland

<sup>2</sup>Department of Evolutional Biology and Environmental Studies, University of Zurich, Switzerland

<sup>3</sup>Finnish Meteorological Institute, Helsinki, Finland

<sup>4</sup>[European Commission](#), Joint Research Centre ([JRC](#)), Ispra, Italy

10 \*These authors contributed equally to this study

Correspondence to: Claudia Guidi ([claudia.guidi@wsl.ch](mailto:claudia.guidi@wsl.ch))

**Abstract.** Predicting soil organic carbon (SOC) stocks and its dynamics in forest ecosystems is crucial for assessing forest C balance, but the relative importance of key controls - litter inputs, climate, and soil properties - remains uncertain. Here, we linked SOC stocks at 556 old-growth Swiss forest sites from 350 to 2000 m a.s.l. to a comprehensive set of environmental 15 variables, encompassing climate (mean annual precipitation, MAP: 700-2100 mm, mean annual temperature, MAT: 0-12°C), soil properties, and forest types. In addition, we compared measured SOC stocks with stocks simulated by the Yasso20-model that is widely used for reporting SOC stock changes. Since Yasso20 is driven solely by litter inputs and climate, deviations between modelled and measured stocks can reveal the significance of additional factors such as organo-mineral interactions that we hypothesized to be crucial for SOC stocks.

20 Total SOC stocks exhibited distinct regional patterns, with the highest values in the Southern Alps, where soils are rich in Fe and Al oxides and receive high MAP. On average, total SOC stocks simulated by Yasso20 aligned well with measured SOC stocks (13.7 vs 13.2 kg C m<sup>-2</sup>). However, the model did not capture regional SOC variability, underestimating SOC stocks by up to 7 kg C m<sup>-2</sup> in the Southern Alps. The underestimation was primarily explained by soil mineral properties with their influence depending on soil pH. In soils with pH ≤ 5, exchangeable Fe had the strongest effect on Yasso20 deviations from 25 measured stocks, while in soils with pH > 5, exchangeable Ca had the strongest effect on model deviations. Beyond Fe and Ca, MAP emerged as an important driver of total SOC stocks, with SOC stocks increasing with MAP. At higher elevation, this coincided with low MAT and a high share of conifers. While Yasso20 accounted for MAT, Yasso20 underestimated SOC stocks for MAP > 1400 mm.

Overall, our results indicate that mineral-driven SOC stabilization and climate are the primary drivers of Yasso20 deviations from measured SOC stocks. Incorporating mineral-driven SOM stabilization and coupling to a soil water model can improve the modeling of SOC stocks. However, further studies are needed to verify how C stabilization mechanisms and soil moisture can be included in model-based estimates of SOC stock changes, which is the primary application of Yasso in greenhouse gas inventories.

## 1 Introduction

Soils are the largest C pool in terrestrial ecosystems, with forest soils storing over 40% of terrestrial ecosystem organic C as soil organic matter (SOM) (Prescott and Grayston, 2023). The complex nature of SOM – comprising a heterogenous mixture of components that turn over on daily to millennial time scales (Sierra et al., 2017; Van Der Voort et al., 2017) – and of processes driving SOM stabilization (Schmidt et al., 2011; Kleber et al., 2015; Lehmann and Kleber, 2015) make it difficult to accurately estimate and predict soil organic carbon (SOC) stocks and its responses to environmental changes (Schrumpf et al., 2011; Smith et al., 2020).

SOC storage is considered to depend mostly on the C input to soils and its transformation and stabilization processes, which are controlled by environmental and biological drivers (Chen et al., 2013; Angst et al., 2018). In temperate forests, SOC storage was shown to be linked to climate, with greater SOC stocks in cool, humid mountainous regions and smaller stocks in warmer and drier regions, as shown in Bavaria (Wiesmeier et al., 2013) and Switzerland (Gosheva et al., 2017). In the German Alps, the increased temperatures during the last three decades have driven topsoil organic C losses in forests with larger losses at low-elevation sites (Prietz et al., 2016). However, geochemical factors may exert a strong additional control on SOC stocks by binding SOC to mineral surfaces, leading to long-term stabilization and SOC accumulation (Hagedorn et al., 2003; Doetterl et al., 2015; Doetterl et al., 2018; Reichenbach et al., 2023). In temperate forest soils, the type and reactivity of soil minerals interacting with SOM were shown to be the principal factor driving SOC accumulation and formation of mineral-associated organic matter, with oxide-dominated soils having a higher capacity to accumulate soil C than soils dominated by phyllosilicate clays (Bramble et al., 2023). For carbonate-containing soils, SOC interactions with  $\text{Ca}^{2+}$ , occlusion within aggregates in Ca-rich substrates and inclusion into carbonates, have been identified as primary SOC stabilization mechanisms (Rowley et al., 2018). In addition to geochemical factors, SOC accumulation is modulated by forest productivity, management intensity and tree species (Bramble et al., 2023), which affect the quantity and quality of litter inputs entering the soil (Vesterdal et al., 2013; Mayer et al., 2020).

While process-based models increasingly integrate SOM-mineral interactions (Abramoff et al., 2018; Abramoff et al., 2022; Brunmayr et al., 2024), SOM stabilization processes are poorly incorporated into models that are used for greenhouse gas (GHG) accounting of the forest soil C balance, which are generally based on data from National Forest Inventories or NFI (Didion et al., 2016; Hernández et al., 2017). Reasons include the poor quantitative knowledge of the complex processes driving SOM storage, and the limited data availability of soil properties at national scale. Simpler soil C models, in contrast,

typically assume that SOC storage is primarily determined by the quantity and quality of litter inputs and climatic conditions, regulating decomposition and stabilization of organic matter (Liski et al., 2005; Ågren et al., 2008). This facilitates their broader applicability. In several European countries including Switzerland, GHG reporting of SOC stock changes in forests is based on model simulations using the soil C cycling model Yasso (Tuomi et al., 2009; Didion et al., 2016; Hernández et al., 2017). The Yasso model was originally developed for forestry applications, relying on data available in forest inventories and basic climate data, without incorporating soil properties (Liski et al., 2005; Tuomi et al., 2009). Currently, the new version of the model (Yasso20) has been calibrated with a more advanced method and using a global SOC dataset (> 4000 measurements), which resulted in an overall better model performance compared to Yasso07 (Viskari et al., 2022).

Here, we aimed to ~~(i) identify the main factors controlling SOC stocks in Swiss forest soils, and to (ii) test the ability of Yasso20 to simulate SOC stocks in forest soils spanning across~~ a large gradient of climate, soil biogeochemistry and forest types ~~across Switzerland~~. ~~To disentangle the main drivers of SOC stocks, our main approach was to (1) simulate SOC stocks in forest soils by Yasso20, make use of the deviations between Yasso simulated (i.e. driven only by litter inputs and climate) and (2) statistically analyze the deviations between Yasso20-simulated and measured SOC stocks. This allows to evaluate the importance of mineral-driven SOC stabilization, since mineral soil properties are not explicitly implemented in Yasso~~ measured SOC stocks to infer the importance of mineral driven SOC stabilization. For this, we analyzed a comprehensive dataset including measured SOC stocks in the organic layers and mineral soil up to 100 cm depth, as well as soil physico-chemical properties for 556 soil profiles located in forests older than 120 years (Gosheva et al., 2017), with an elevation ranging from 370 to 1960 m a.s.l. The dataset covered a wide range of climatic conditions (mean annual precipitation of 700-2100 mm, mean annual temperature 0-12 °C), soil properties (i.e. pH 3-8) and forest types. The dataset included soil physico-chemical characteristics such as clay content, pH, exchangeable Fe, Al, and Ca, topographic attributes, tree species composition, and satellite-derived NPP. Given that the soil C model Yasso20 accounts only for litter inputs and climatic conditions, we hypothesised that mineral soil components driving SOM stabilization (e.g. Fe, Al, and Ca content) would largely explain the deviations between simulated and measured SOC stocks. In turn, this would imply that mineral-driven C stabilization is a key process for soil C storage at the regional and national scale which should be considered in models used for GHG reporting.

## 2 Methods

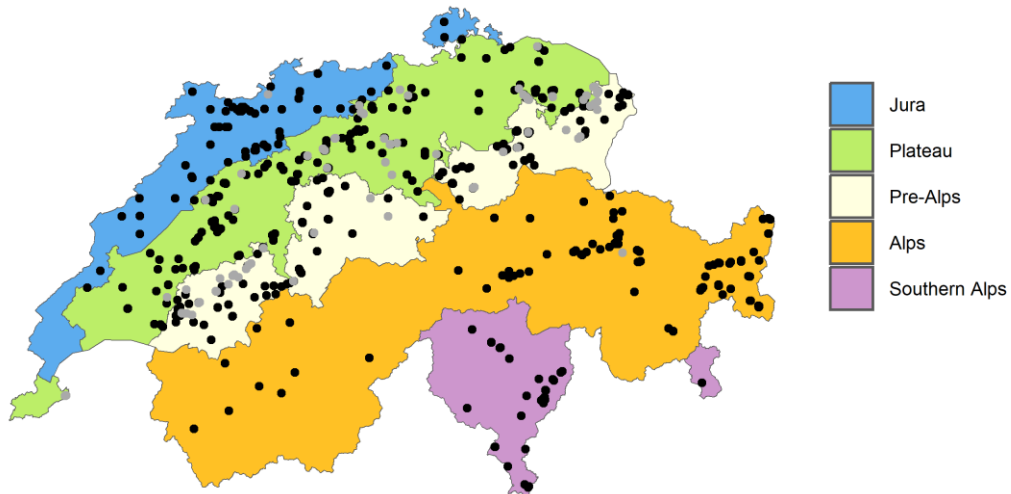
### 2.1 Study area and sampling sites

For our study, we considered 556 sites in old-growth forests i.e. forests older than 120 years (Fig. 1; 52% broadleaf- vs 48% conifer-dominated sites) from a soil database encompassing approximately 1000 soil profiles (Gosheva et al., 2017). In combination with the typically small-scale, ~~single tree based~~ management in Switzerland, ~~which includes planned loggings of single trees with harvesting residues (e.g. fine branches, foliage, belowground part with trunk to approx. 30 cm aboveground) normally left in the stand (Brändli et al., 2020)~~, the focus on old forests ensures that there have been only

95 minimal reduced disturbances in the forest cover over the past decades. Although natural disturbances such as windthrows occurred in Swiss forests (e.g. Vivian in 1990 and Lothar in 1999) with possible impact on SOC stocks (Mayer et al., 2023),

95 none of the forest sites was affected as sampling excluded windthrow sites. Forests in Switzerland can be divided into five major **biogeographic**-regions (Fig. 1) according to Fischer and Traub (2019) with relatively uniform growth, specific soil properties and forest types (Gosheva et al., 2017).

100 Most of our sites are located in the Swiss Plateau ( $n = 164$ ), a region characterized by more or less deeply decarbonated soils from still calcareous moraines and tertiary sediments (molasse), followed by sites in the Pre-Alps ( $n = 138$ ), a region consisting of soils with highly variable weathering and decalcification depths from very different types of sediments (Gnägi and Labhart, 2015). The remaining sites are in the Alps ( $n = 81$ ) on heterogeneous bedrock, in the Jura ( $n = 54$ ) dominated by limestone or marl, and in the Southern Alps ( $n = 31$ ) with mainly gneiss as bedrock (Gnägi and Labhart, 2015). Waterlogged soils (i.e. redoximorphic soils, characterized by the periodic or permanent oxygen shortage) were studied separately ( $n = 88$ ), since excess moisture dominates soil development and SOM stabilization mechanisms at these soils.



105

**Figure 1: Distribution of the sampled forest sites (total  $n$  sites = 556, of which  $n = 88$  waterlogged soils shown in grey) in the five **biogeographic**-regions of Switzerland. Note that the Alps have fewer sites since largely un-forested (i.e. above the treeline).**

## 2.2 Soil sampling and analysis, climate and topography

110 The 556 soil profiles were sampled from 1989 to 2004 by genetic horizons up to the parent material. Composite soil samples were taken from the front wall of the soil profiles (over an average width of 70 cm). Samples were dried at 60°C and sieved with a 2-mm mesh before chemical analysis. Soil type was classified according to the World Reference Base (Iuss, 2007).

115 Total and organic C contents were measured in ground samples by dry combustion using an elemental analyzer (NC 2500, CE Instruments, Italy). Soil samples with pH > 6 were first treated with HCl to remove inorganic C prior to dry combustion (Walthert et al., 2010). Soil texture was characterized by measuring the clay, silt and sand contents using the sedimentation method according to Gee and Bauder (1986). Soil pH was measured potentiometrically in a 0.01 M CaCl<sub>2</sub> solution. Contents of exchangeable Al, Fe, and Ca (in mmolc kg<sup>-1</sup>) were obtained by 1 M ammonium chloride extraction (Walthert et al., 2004). Soil properties were calculated for 0-30 cm and 0-100 cm depth intervals of the mineral soil by weighted averages of their contents according to the amount of fine earth in the various soil horizons.

120 Data on elevation and slope were determined from a 25-m digital elevation model for all sites (Swisstopo, 2011). Slope orientation and topography were assessed during the soil surveys. Annual climate data for each site (mean monthly temperature and mean monthly precipitation for the period 1961-1990) were obtained from the gridded data produced by the Swiss Federal Office of Meteorology and Climatology (Meteoswiss, 2024). The Braun-Blanquet cover abundance scale (Braun-Blanquet, 1964) was used to quantify plant species cover in an area ranging from 100 to 500 m<sup>2</sup> (Walthert et al., 125 2013). Percentage of broadleaf tree species was calculated as the sum of the cover of all broadleaf species divided by the sum of the cover of all tree species at the tree level. Only for visualization purposes, the forest sites were subdivided into two types based on the broadleaf percentage: coniferous (0-50%) and broadleaf (51-100%) forests.

### 2.3 Calculation of SOC stocks from sampled soil profiles

130 SOC stocks were calculated separately for the organic layers including L (undecomposed litter), F (fermentation) and H (humified) horizons and the mineral soil at 0-100 cm depth. Total SOC stock is the sum of stocks in the organic layers and in the mineral soil. SOC stocks in the organic layer were calculated according to Hagedorn et al. (2010), with the mass of the organic layer calculated as the product of the density (L: 0.10 g cm<sup>-3</sup>, F: 0.15 g cm<sup>-3</sup>, H: 0.20 g cm<sup>-3</sup>) and the volume (based on measured thickness), multiplied by the percentage of C content obtained by dry combustion (see section 2.2). Mineral SOC stocks were calculated using the following Eq. (1):

$$135 SOC(h, z) = \sum_1^z (h_i (1 - \theta_i) \rho_i C_i) \quad (1)$$

where  $SOC(h, z)$  represents SOC stocks (kg C m<sup>-2</sup>) of all the  $z$  mineral soil horizons,  $C_i$  - the organic carbon content of the horizon  $i$  (kg kg<sup>-1</sup> of C) obtained by dry combustion,  $\rho_i$  is the density of the fine earth (g cm<sup>-3</sup>),  $\theta_i$  is the volumetric stone content (m<sup>3</sup> m<sup>-3</sup>) visually estimated from the soil profile (Richard et al., 1978), and  $h_i$  is the horizon thickness (m). A pedotransfer function (PTF) based on a calibration dataset of 559 mineral soil horizons from 134 different Swiss forest sites 140 and a validation set of 131 horizons from 34 sites, was used to estimate the density of the fine earth fraction (Nussbaum et al., 2016). Covariates used in this PTF are sampling depth, slope, field estimates of stone content and soil density, biogeographic region, and organic C content.

## 2.4 Input derivation and SOC stocks simulations with Yasso20

SOC stock simulations were conducted with the soil C cycling model Yasso20. The model was calibrated by Viskari et al. (2022) using several datasets describing different processes of the soil C cycle, including litterbag decomposition time series, a woody decomposition dataset and global SOC stock measurements, which make Yasso20 potentially suitable for a wide range of environmental conditions. Based on litter input data (i.e., foliage, deadwood etc.), Yasso20 simulates flows of C between four chemical classes of C compounds and a humus ("H") pool representing long-lived, stable SOC as a function of temperature and precipitation. Litter inputs are sub-divided into the following four different chemical C compounds that are the same as the SOC classes in the model: "A" represents hydrolysable compounds in acid, "W" water-soluble compounds, "E" ethanol-soluble compounds, and "N" non-soluble compounds. Each of these compounds have different C decomposition rates. The sum of the AWEN compound classes (representing the "labile" C pools) and the H pool (the "stable" C pools) corresponds to the total "simulated" SOC stocks, including the SOC stored in the organic layers plus in the mineral soil up to 100 cm depth. Parameters defining C decomposition rates and C cycling between C compartments and to a more stable H pool are obtained probabilistically using Markov Chain Monte Carlo sampling (Viskari et al., 2022) and are fitted based on data from several litterbag studies (Berg et al., 1991; Trofymow, 1998; Gholz et al., 2000), woody litter decomposition experiments (Mäkinen et al., 2006), and global SOC measurements from Oak Ridge National Laboratory (Zinke et al., 1986).

To obtain a proxy of site-specific litter inputs for Yasso20 simulations, we derived the average net primary production (NPP) for the period 2001-2022 from Terra and Aqua MODIS-satellite at 500-m resolution (Running and Zhao, 2021a, b), with a maximum NPP to GPP (gross primary production) ratio of 0.5 (Viskari et al., 2022). We partitioned the NPP into broadleaf and conifer species, multiplying the NPP by the percentage of broadleaf and conifer species recorded by field assessments at each site. Then, we divided the NPP into different tree components, multiplying the NPP by average tree allocation factors (stem: 0.30; branches: 0.04; twigs: 0.03; coarse roots: 0.11; fine roots: 0.15; foliage: 0.27; seeds: 0.10) derived from 15 years of tree growth data at 18 long-term forest ecosystem research (LWF) sites across Switzerland (Etzold et al., 2014). Fine roots and foliage represented the group of non-woody litter, whereas woody litter included stem wood, branches, twigs, coarse roots, and seeds. The C inputs for each pool were separated into the four AWEN ~~compounds~~ components according to the percentage of broadleaf and conifer species at each site, using the functions and approach adopted in the Swiss GHG inventory (Didion, 2023) following experimentally derived based on measured fractions at LWF sites of the long-term forest monitoring program LWF in Switzerland (Didion et al., 2014). Data for observed climate were obtained for each site (30-year average climate, 1961-1990) from spatially gridded data of the Federal Office of Meteorology and Climatology MeteoSwiss (Meteoswiss, 2024), see *section 2.2*.

The Yasso20 simulations were performed in R ([www.r-project.org](http://www.r-project.org)) version 4.2.2 (R Core Team, 2022) with the package *Ryassofortran*, version 0.4.0 (Pusa, 2023). Average litter input derived from NPP and climate data were used with spin-up simulations to reach theoretical steady-state SOC stocks (Mao et al., 2019), assuming that current SOC stocks have

accumulated over centuries (Gimmi et al., 2013). At each site, independent simulations were based on 500 randomly-sampled parameter vectors to represent uncertainty related to model parameters (Viskari et al., 2022).

## 2.5 Statistical analysis

All statistical analyses were performed with R version 4.2.2 (R Core Team, 2022). To summarize the correlated 180 numerical explanatory variables into larger groups, we performed a principal component analysis (PCA) including all the numerical variables (pH, clay content, exchangeable contents of Fe, Al, and Ca, mean annual temperature or MAT, mean annual precipitation or MAP, NPP, percentage of broadleaves and slope) with scaled variables. Only principal components with eigenvalues  $>1$  were retained (Kaiser-Guttman criterion).

The effects of (i) main principal components, and (ii) soil physico-chemical properties (pH, clay content, exchangeable 185 contents of Fe, Al, and Ca) in the upper 30 cm mineral soil - the most relevant depth for tree rooting, litter decomposition processes and organic layer development - and site variables (MAT, MAP, NPP, percentage of broadleaves and slope) on total SOC stocks and Yasso20 deviations (simulated minus measured values of total SOC stocks) were tested using linear

190 mixed-effect models with the *nlme* package, version 3.1–160 (Pinheiro et al., 2022). [Statistical analysis of Yasso20 deviations allows to assess effects of the main drivers of SOC stocks on model discrepancies from measured values](#). In order

195 to account for a small spatial autocorrelation in the model residuals, the ~~biogeographic~~ region was included as a random intercept in the model, which allowed to estimate an overall effect of the linear model (i.e. model estimate). Effects of explanatory variables on SOC stocks were also tested for each ~~biogeographic~~ regions by linear models. To meet the assumption of normally distributed residuals, the numerical explanatory variables were log- or square-root transformed when necessary, which ensured a linear relationship between the explanatory and the response variable. Then, all explanatory

195 variables were ~~standardized\_centered~~ to a mean of 0. The assumption of normal distribution of residuals was verified through quantile–quantile plots and plots of residuals vs fitted values. Based on existing literature, the variables pH, clay content, exchangeable Fe, Al, and Ca, MAT, MAP, NPP, percentage of broadleaves and slope were identified as key drivers of SOC stocks and thus as explanatory variables. Exchangeable Al was excluded from the final statistical model due to its strong correlation with pH and exchangeable Fe ( $r = -0.93$  and  $+0.87$ , respectively). Exchangeable Fe was retained as the primary

200 proxy for pedogenic oxides (Fig. [S4S6](#)). For the statistical analysis of Yasso20 deviations, NPP was excluded from the final model since it was used as main input of the soil C cycling model Yasso20. Two-way interactions between climate and soil properties (i.e. exchangeable contents of Fe, Ca, clay content, and pH) and between soil properties and pH were also tested (Table S2, Table S3), since interactions of climate and geochemical factors are known to drive SOC storage (Doetterl et al., 2015).

205 Measured vs simulated SOC stocks by ~~biogeographic~~ regions and forest types were compared using Welch's *t*-tests, after verifying normality assumptions. Correlations between simulated and measured SOC stocks were tested using Pearson's product moment correlation coefficient ( $r$ ), which agreed well with Spearman's rank correlation coefficient (*not shown*).

### 3 Results

#### 3.1 Site characteristics

210 Distinct site characteristics were found in each of the five **biogeographic**-regions of Switzerland (Fig. 1, Table 1). Topsoils in the Jura showed the highest pH, as well as contents of clay and Ca, while the most acidic soils were found in the Southern Alps, with highest contents of exchangeable Fe, oxalate-extractable Fe and Al (Table 1). MAP was highest in the Southern Alps and the Pre-Alps, whereas the Plateau had the highest MAT (Table 1) and NPP (Fig. S1a). Under conifer-dominated forests, topsoils were more acidic (average pH  $\pm$  standard error at 0-30 cm depth, conifers:  $4.7 \pm 0.1$  vs 215 broadleaves  $5.2 \pm 0.1$ ) and had higher contents of exchangeable Fe and Al than broadleaf-dominated forests (*data not shown*).

220 **Table 1: Average values of soil properties (pH, clay content, exchangeable contents of Fe, Al, and Ca) in the upper 30 cm of mineral soil, annual climate data (MAT = mean annual temperature, MAP = mean annual precipitation), net primary production (NPP) from MODIS (average 2001-2022), and elevation in the 556 sites across the five **biogeographic**-regions of Switzerland, with waterlogged soils shown separately. For a subset of sites ( $n = 123$ ), oxalate-extractable Fe and Al ( $Fe_{ox}$  and  $Al_{ox}$ ) in the upper 30 cm of mineral soil are reported. Values are means with standard errors in brackets.**

	Jura	Plateau	Pre-Alps	Alps	Southern Alps	Waterlogged	Switzerland
All sites	$n = 54$	$n = 164$	$n = 138$	$n = 81$	$n = 31$	$n = 88$	$n = 556$
pH	6.2 (0.2)	4.7 (0.1)	4.8 (0.1)	5.3 (0.2)	4.3 (0.2)	5.3 (0.2)	5.0 (0.1)
Clay (%)	35.5 (1.9)	19.6 (0.7)	24.0 (1.0)	17.2 (1.1)	12.8 (1.7)	25.3 (1.2)	22.4 (0.5)
$Fe_{exch}$ (mmolc kg $^{-1}$ )	0.2 (0.1)	0.5 (0.1)	0.9 (0.1)	0.6 (0.1)	1.3 (0.3)	0.6 (0.1)	0.7 (0.0)
$Al_{exch}$ (mmolc kg $^{-1}$ )	7.2 (2.2)	28.7 (2.3)	39.6 (4.3)	18.0 (2.8)	35.1 (4.9)	21.8 (4.1)	27.0 (1.6)
$Ca_{exch}$ (mmolc kg $^{-1}$ )	302.0 (23.6)	73.1 (8.3)	116.6 (12.3)	122.5 (11.8)	48.9 (17.9)	138.2 (12.1)	122.3 (6.0)
MAT (°C)	7.0 (0.2)	8.0 (0.0)	6.4 (0.1)	3.9 (0.3)	6.6 (0.5)	7.0 (0.2)	6.7 (0.1)
MAP (mm)	1253 (30)	1141 (11)	1508 (22)	1021 (28)	1579 (47)	1329 (28)	1279 (12)
NPP (kg C m $^{-2}$ yr $^{-1}$ )	0.64 (0.01)	0.65 (0.01)	0.61 (0.01)	0.45 (0.01)	0.57 (0.03)	0.63 (0.01)	0.60 (0.01)
Elevation (m)	789 (31)	592 (10)	906 (24)	1427 (41)	1027 (87)	789 (34)	866 (16)
Subset sites	$n = 10$	$n = 52$	$n = 21$	$n = 12$	$n = 11$	$n = 17$	$n = 123$
$Fe_{ox}$ (g kg $^{-1}$ )	2.23 (0.32)	2.79 (0.22)	4.38 (0.77)	5.89 (1.28)	9.13 (2.68)	4.43 (0.46)	4.11 (0.36)
$Al_{ox}$ (g kg $^{-1}$ )	2.18 (0.36)	2.05 (0.23)	2.68 (0.40)	2.23 (0.47)	6.52 (1.47)	1.99 (0.23)	2.58 (0.22)

225 NPP peaked at an elevation of about 700 m a.s.l., then decreased with increasing elevation (linear model fit for elevation  $> 700$  m:  $-0.26 \pm 0.01$  kg C m $^{-2}$  yr $^{-1}$  per 1000 m elevation gain;  $R^2 = 0.65$ ,  $P < 0.001$ , Fig. 2a). In contrast to NPP, SOC stocks in the organic layer increased with elevation ( $3.5 \pm 0.4$  kg C m $^{-2}$  per 1000 m increase in elevation;  $R^2 = 0.14$ ,  $P < 0.001$ ; Fig. 2b) in sites excluding waterlogged soils ( $n = 468$ ). In the mineral soil, SOC stocks were not related to elevation (Fig. 2c), thus the ratio between SOC stored in the organic layer and in the mineral soil increased with elevation. NPP was negatively correlated to organic layer SOC stocks ( $R^2 = 0.08$ , with Pearson correlation coefficient  $r = -0.29$ ,  $P < 0.001$ ), while positively 230 but weakly related to mineral SOC stocks ( $R^2 = 0.01$ , with Pearson correlation coefficient  $r = +0.12$ ,  $P = 0.006$ ).

The first three principal components of the PCA with soil physico-chemical variables and site properties explained 74% of variance in the data (Table S1a). The first PC (PC1) was characterized by high loadings of soil chemical parameters: pH (0.48), Ca (0.47), Al (-0.43), and Fe (-0.40), explaining 35% of the variance. PC2 (24% of variance) showed high loadings of MAT (0.58), NPP (0.58), and broadleaf percentage (0.44), whereas PC3 (15% of variance) of MAP (0.63) and clay content 235 (0.44) (Table S1a).

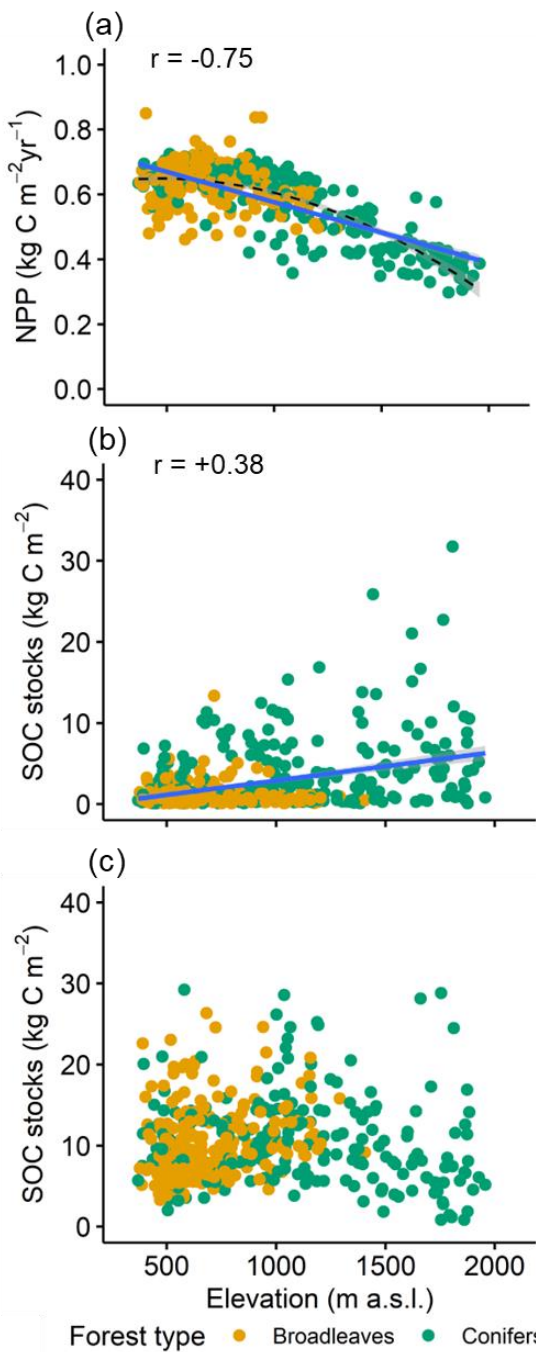
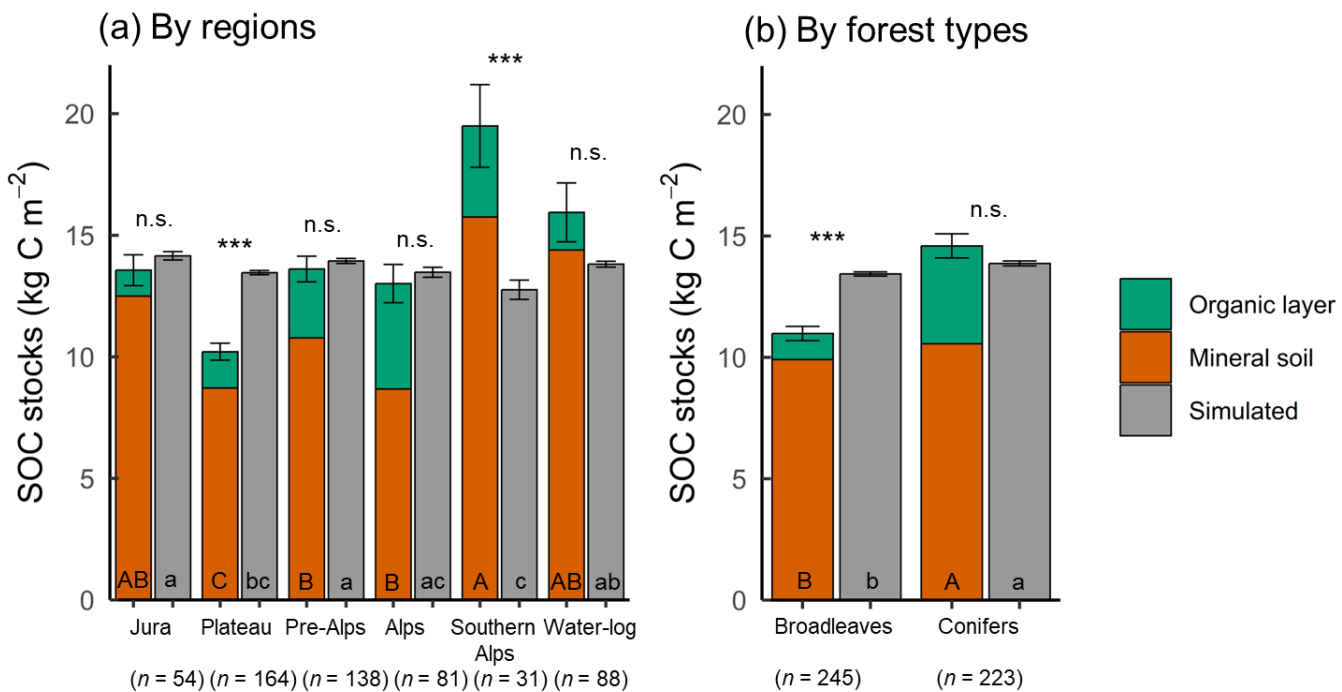


Figure 2: Net primary production (NPP) from MODIS (average 2001-2022) (a), SOC stocks in the organic layers (b), and in the mineral soil at 0-100 cm depth (c) against elevation in 468 forest sites across Switzerland (excluding waterlogged soils). Plotted lines show significant linear correlations ( $P < 0.05$ ) with 95% confidence intervals in grey and the Pearson correlation coefficient ( $r$ ). A polynomial regression is also shown as dotted line in (a).

### 3.2 Measured and simulated SOC stocks

Measured SOC stocks were highest in the Southern Alps ( $19.5 \pm 1.7 \text{ kg C m}^{-2}$ ) followed by the Pre-Alps, Jura, and the Alps, while lowest in the Plateau ( $10.2 \pm 0.3 \text{ kg C m}^{-2}$ , Fig. 3a). On average, the Yasso20-simulated SOC stocks were similar to the measured stocks at the 556 sites including waterlogged soils (average  $\pm$  standard error; simulated  $13.7 \pm 0.1$  vs measured  $13.2 \pm 0.3 \text{ kg C m}^{-2}$ , Welch's  $t$ -test:  $P = 0.16$ ). Waterlogged soils had SOC stocks of  $15.9 \pm 1.2 \text{ kg C m}^{-2}$ , and are thus considered separately in further analyses. In comparison to measured stocks and despite the large NPP range across regions (Fig. S1a), simulated SOC stocks differed only little among the biogeographic-regions (Fig. 3a, Fig. S1b). The largest deviations between simulated and measured SOC stocks were observed in the Southern Alps, where Yasso20 underestimated stocks by almost  $7 \text{ kg C m}^{-2}$  (-35% of measured SOC stocks, Welch's  $t$ -test:  $P < 0.001$ , Fig. 3a). In contrast, Yasso20 overestimated SOC stocks by about  $3 \text{ kg C m}^{-2}$  in the Plateau (+33% of measured SOC stocks,  $P < 0.001$ ). The simulations for the Jura, Pre-Alps and Alps agreed well with SOC measurements, with average deviations below  $1 \text{ kg C m}^{-2}$  (2-4% of measured SOC stocks,  $P > 0.05$ ). In waterlogged soils, Yasso underestimated SOC stocks by about  $2 \text{ kg C m}^{-2}$  (-13% of measured SOC stocks,  $P = 0.08$ ).



**Figure 3: Comparison between measured SOC stocks vs Yasso20-simulated stocks by: (a) biogeographic-regions of Switzerland, with waterlogged soils shown separately, and (b) forest types, excluding waterlogged soils. The measured stocks are shown as organic layers and mineral soils to 100 cm depth (total  $n$  sites = 556; excluding waterlogged soils,  $n$  sites = 468). The simulated stocks at each site are based on the mean of 500 replicate simulations representing model parameters uncertainty. SOC stocks are represented as means  $\pm$  standard errors.  $P$ -values are calculated with Welch's  $t$ -tests:  $P \geq 0.05$  (n.s., not significant),  $P < 0.001$  (\*\*\*) and  $P < 0.05$  (\*\*\*\*). Capital letters indicate significantly different means among measured SOC stocks, while lowercase letters indicate not significantly different means.**

significantly different means among Yasso20-simulated SOC stocks, based on ANOVA followed by Tukey's test (Fig. 3a) and Welch's t-tests (Fig. 3b) with  $P < 0.05$ .

Measured SOC stocks were greater in conifer- than in broadleaf-dominated stands ( $14.6 \pm 0.5$  vs  $11.0 \pm 0.3$  kg C m $^{-2}$ ) respectively, without waterlogged soils; Fig. 3b), mostly due to higher SOC stocks in the organic layers (+3 kg C m $^{-2}$ ). 265 However, differences in Yasso20-simulated SOC stocks Yasso20 estimated similar total SOC stocks in between conifer- and broadleaf-dominated forests were more limited ( $13.9 \pm 0.1$  vs  $13.4 \pm 0.1$  kg C m $^{-2}$ , respectively), overestimating with an overestimation of SOC stocks in broadleaf forests by  $2.5$  kg C m $^{-2}$  (Welch's  $t$ -test:  $P < 0.001$ , Fig. 3b) while a slightly underestimating underestimate of SOC stocks in conifer forests by less than  $1$  kg C m $^{-2}$  ( $P = 0.16$ , Fig. 3b).

### 270 3.3 Drivers of SOC stocks and Yasso20 deviations

SOC stocks were positively correlated with MAP ( $r = +0.32$ ,  $P < 0.001$ , Fig. 4f), and negatively correlated with MAT ( $r = -0.17$ ,  $P < 0.001$ , Fig. 4g). Since the reactivity of mineral surfaces is pH dependent, we We separated the dataset into soils with  $pH \leq 5$  and with  $pH > 5$ , since pH is recognized as a predictor of SOC stabilization mechanisms, mediated by Al- or Fe-under acidic conditions while Ca exerts a dominant influence under increasing pH (Rowley et al., 2018). Consistently, 275 wWith  $pH \leq 5$ , SOC stocks increased with increasing content of exchangeable Fe and Al ( $r = +0.60$  and  $r = +0.38$ , respectively, with  $P < 0.001$ , Fig. 4b,c), while when pH was above 5, SOC stocks increased with increasing exchangeable Ca ( $r = +0.49$ ,  $P < 0.001$ , Fig. 4d).

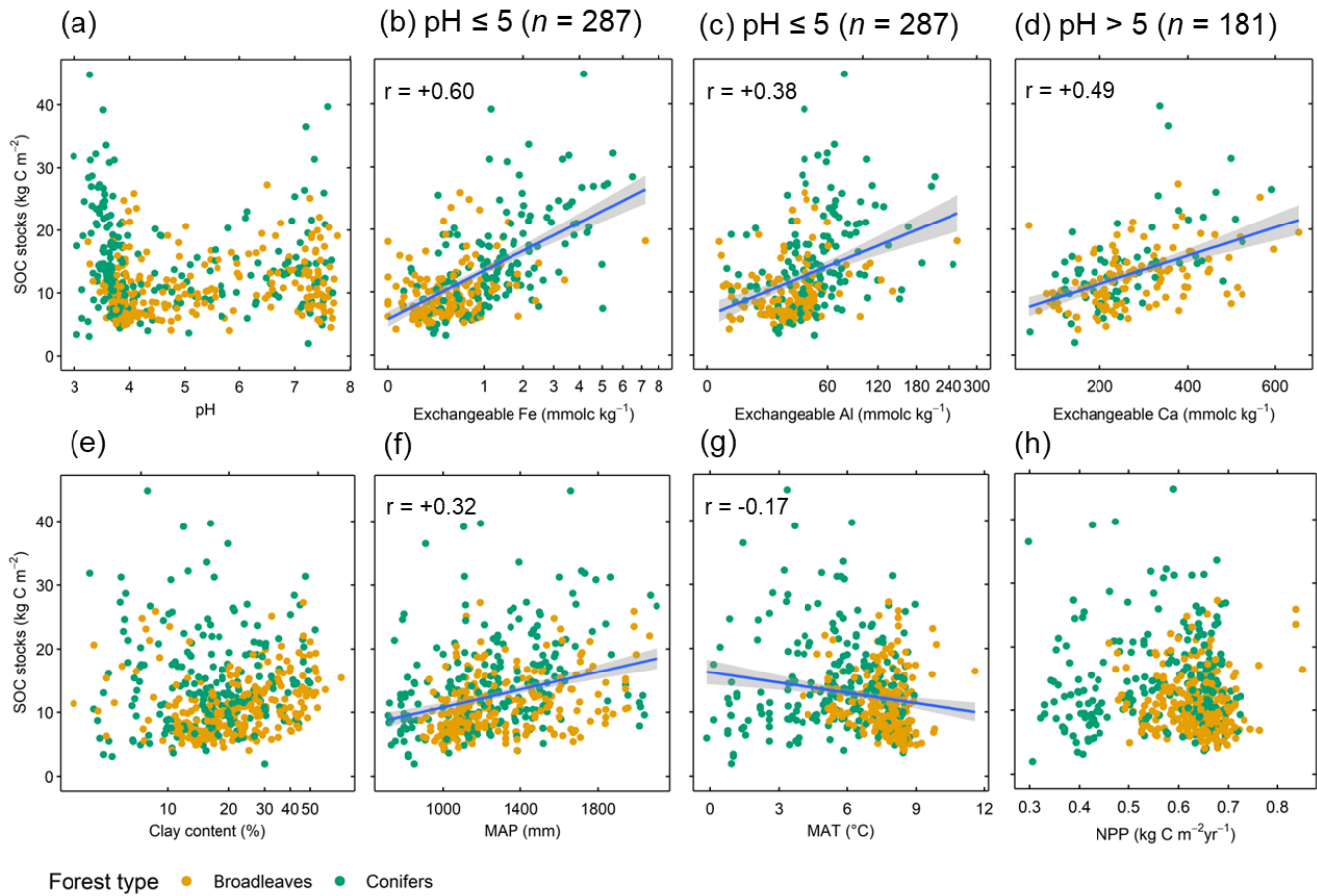


Figure 4: Correlations between total SOC stocks and selected soil properties (exchangeable Fe and Al are shown on a square-root scale axis, clay on a natural-logarithm scale axis) and site variables (MAP = mean annual precipitation; MAT = mean annual temperature; NPP = net primary production). Total  $n$  sites = 468 (waterlogged soils excluded). Plotted lines show significant linear correlations ( $P < 0.05$ ) with 95% confidence intervals in grey and the Pearson correlation coefficient ( $r$ ).

The principal components PC1 (including primarily soil chemical parameters) and PC3 (including MAP and clay) had a significant effect on SOC stocks (Table S1b). In comparison, PC2 (with MAT, NPP and forest type) was statistically unrelated with SOC stocks (Table S1b). We then tested effects of soil properties and site variables on SOC stocks ( $n = 468$  sites, waterlogged soils excluded, Table 2). Linear mixed-effect models, including a random intercept for the region, showed a significant overall effect of exchangeable Fe, pH, MAP, broadleaf percentage and slope on total SOC stocks. We found a positive interaction between pH and exchangeable Ca (Table S2, model with interactions), with exchangeable Ca enhancing SOC storage stocks at pH  $> 5$  (Fig. S2bS4b). Additionally, there was a significant, negative interaction of clay and MAP (Table S2, Fig. S2aS4a) that mostly reflected SOC-rich soils in the Southern Alps with high MAP but low clay content (Table 1). In soils with pH  $\leq 5$  ( $n = 287$ ), the exchangeable Fe and MAP had a positive effect on SOC stocks, while slope and clay content had a negative effect on SOC stocks (Table 2). In soils with pH  $> 5$  ( $n = 181$ ), exchangeable Ca and MAP

had a positive impact on SOC stocks, while broadleaf percentage and slope decreased SOC stocks. Analysis of drivers of SOC stocks within **biogeographic**-regions (Table S5) indicated that exchangeable Fe explained the largest proportion of model variance (from 30 to 46% of total  $R^2$ ) for all **biogeographic**-regions except the Jura, characterized by average pH > 6, where exchangeable Ca explained the highest amount of variation (44% of total  $R^2$ ).

**Table 2: Drivers of total SOC stocks. Effects of soil properties in the upper 30 cm mineral soil (i.e. pH, clay content, exchangeable contents of Fe and Ca), MAT (mean annual temperature), MAP (mean annual precipitation), NPP (net primary production), percentage of broadleaves and slope on total SOC stocks ( $\text{kg C m}^{-2}$ ). Linear mixed-effect models with region as random intercept were developed for (i) all sites excluding waterlogged soils, (ii) sites with  $\text{pH} \leq 5$ , and (iii) sites with  $\text{pH} > 5$ .**

	All sites ( $n = 468$ )				pH $\leq 5$ ( $n = 287$ )				pH $> 5$ ( $n = 181$ )					
	Est.	SE	t	P	Est.	SE	t	P	Est.	SE	t	P		
(Intercept)	13.73	1.15	12.0	<b>&lt;0.001</b>	(Intercept)	13.09	0.84	15.6	<b>&lt;0.001</b>	(Intercept)	14.31	1.81	7.9	<b>&lt;0.001</b>
pH	1.81	0.31	5.8	<b>&lt;0.001</b>	pH	2.03	1.23	1.6	0.10	pH	-0.24	0.55	-0.4	0.67
log(Clay)	0.12	0.59	0.2	0.84	log(Clay)	-2.49	0.78	-3.2	<b>0.002</b>	Clay	0.02	0.04	0.4	0.69
sqrt(Fe)	6.64	0.68	9.7	<b>&lt;0.001</b>	sqrt(Fe)	7.19	0.85	8.5	<b>&lt;0.001</b>	sqrt(Fe)	1.53	3.43	0.4	0.66
log(Ca)	0.20	0.25	0.8	0.42	log(Ca)	0.19	0.29	0.6	0.52	Ca	0.03	0.00	5.8	<b>&lt;0.001</b>
MAT	-0.02	0.21	-0.1	0.92	MAT	-0.24	0.27	-0.9	0.39	MAT	0.59	0.30	2.0	0.05
MAP	<b>0.04</b>	<b>0.00</b>			MAP	<b>0.04</b>	<b>0.00</b>			MAP	<b>0.00</b>	<b>0.00</b>		
	<b>0.64</b>	<b>0.12</b>	5.5	<b>&lt;0.001</b>		<b>0.94</b>	<b>0.15</b>	6.4	<b>&lt;0.001</b>		<b>0.44</b>	<b>0.17</b>	2.6	<b>0.010</b>
NPP	2.09	4.37	0.5	0.63	NPP	6.01	5.21	1.2	0.25	NPP	-13.24	6.83	-1.9	0.05
Broadleaf%	-0.02	0.01	-2.9	<b>0.004</b>	Broadleaf%	-0.01	0.01	-1.2	0.21	Broadleaf%	-0.03	0.01	-2.5	<b>0.014</b>
sqrt(Slope%)	-0.34	0.11	-3.2	<b>0.001</b>	sqrt(Slope%)	-0.53	0.14	-3.8	<b>&lt;0.001</b>	Slope%	-0.03	0.01	-2.3	<b>0.022</b>
DF	454					273					167			
marginal $R^2$	0.30					0.48					0.24			
conditional $R^2$	0.44					0.53					0.57			
RMSE												4.3		
( $\text{kg C m}^{-2}$ )	4.9					4.6								

Model estimates (Est.), standard errors (SE), t statistic and  $P$ -values are reported ( $P < 0.05$  highlighted in bold).

Measurement units of independent variables are reported in Table 1. [For result interpretation, MAP is here reported in 100 mm unit.](#)

DF is the degrees of freedom. Marginal  $R^2$  includes the variance of the fixed effects, while conditional  $R^2$  both the fixed and random effects calculated with the R package *performance* (Lüdecke et al., 2021).

RMSE is the root mean squared error.

Similarly to SOC stocks, Yasso20 deviations (i.e. difference between Yasso20-simulated and measured SOC stocks, with positive deviations indicating a model overestimation of SOC stocks, while negative deviations a model underestimate,  $n = 468$  sites, Table 3) were significantly affected by exchangeable Fe, pH, MAP, broadleaf percentage, and slope. Although the correlation between MAT and the Yasso20 deviations is overall positive ( $r = +0.10$ , see Fig. [S3S5g](#)), the random intercept for the different regions – which accounts for the regional variability - led to a negative estimated linear effect of MAT on Yasso20 deviations.

**Table 3: Drivers of Yasso20 deviations. Effects of soil properties in the upper 30 cm mineral soil (i.e. pH, clay content, exchangeable contents of Fe and Ca), MAT (mean annual temperature), MAP (mean annual precipitation), percentage of broadleaves and slope on Yasso20 deviations (simulated minus measured values of total SOC stocks) in  $\text{kg C m}^{-2}$ . Linear mixed-effect models with region as random intercept were developed for (i) all sites excluding waterlogged soils, (ii) sites with  $\text{pH} \leq 5$ , and (iii) sites with  $\text{pH} > 5$ .**

	All sites ( <i>n</i> = 468)				pH ≤ 5 ( <i>n</i> = 287)				pH > 5 ( <i>n</i> = 181)					
	Est.	SE	t	P	Est.	SE	t	P	Est.	SE	t	P		
(Intercept)	-0.26	1.39	-0.2	0.85	(Intercept)	0.42	1.02	0.4	0.68	(Intercept)	-1.30	2.58	-0.5	0.62
pH	-1.78	0.32	-5.6	<b>&lt;0.001</b>	pH	-1.99	1.25	-1.6	0.11	pH	-0.03	0.59	0.0	0.96
log(Clay)	0.24	0.60	0.4	0.69	log(Clay)	2.64	0.79	3.4	<b>&lt;0.001</b>	Clay	0.01	0.04	0.2	0.87
sqrt(Fe)	-6.68	0.70	-9.6	<b>&lt;0.001</b>	sqrt(Fe)	-7.24	0.86	-8.4	<b>&lt;0.001</b>	sqrt(Fe)	-4.74	3.63	-1.3	0.19
log(Ca)	-0.38	0.25	-1.5	0.12	log(Ca)	-0.34	0.29	-1.2	0.24	Ca	-0.03	0.00	-5.2	<b>&lt;0.001</b>
MAT	-0.51	0.18	-2.9	<b>0.004</b>	MAT	-0.43	0.24	-1.8	0.07	MAT	-0.66	0.25	-2.6	<b>0.009</b>
MAP	<b>-0.58</b>	<b>0.12</b>			MAP	<b>-0.91</b>	<b>0.15</b>			MAP	<b>-0.29</b>	<b>0.17</b>		
	<b>0.01</b>	<b>0.00</b>	-5.0	<b>&lt;0.001</b>		<b>0.01</b>	<b>0.00</b>	-6.2	<b>&lt;0.001</b>		<b>0.00</b>	<b>0.00</b>	-1.7	0.09
Broadleaf%	0.03	0.01	3.2	<b>0.0017</b>	Broadleaf%	0.02	0.01	1.5	0.14	Broadleaf%	0.03	0.01	2.7	<b>0.009</b>
sqrt(Slope)	0.36	0.11	3.3	<b>0.001</b>	sqrt(Slope)	0.52	0.14	3.6	<b>&lt;0.001</b>	Slope	0.03	0.02	2.2	<b>0.026</b>
DF	455				274						168			
marginal R <sup>2</sup>	0.25				0.43						0.17			
conditional R <sup>2</sup>	0.45				0.52						0.66			
RMSE	5.0				4.7						4.6			
(kg C m <sup>-2</sup> )														

320 Model estimates (Est.), standard errors (SE), t statistic and *P*-values are reported (*P* < 0.05 highlighted in bold).

Measurement units of independent variables are reported in Table 1. [For result interpretation, MAP is here reported in 100 mm unit.](#)

DF is the degrees of freedom. Marginal R<sup>2</sup> includes the variance of the fixed effects, while conditional R<sup>2</sup> both the fixed and random effects calculated with the R package *performance* (Lüdecke et al., 2021).

RMSE is the root mean squared error.

320

## 325 4 Discussion

### 4.1 Soil properties are the primary drivers of SOC stocks

Our study along large environmental gradients from temperate to alpine old forest stands across Switzerland indicated that soil mineral properties, together with climate, play a dominant role in controlling SOM stabilization and SOC stocks.

This finding aligns with a global scale study that demonstrated the primary influence of soil properties, alongside climate, in

330

driving SOC stocks across whole-soil profiles (Luo et al., 2021). Overall, exchangeable Fe was the predictor with strongest effect on SOC stocks within [biogeographic](#) regions with acidic topsoil (Table S5). The SOC stocks were greatest in the Southern Alps, having a slightly lower NPP than the Swiss average but higher contents of exchangeable Fe and Al (Table 1). Moreover, the comparison of SOC stocks simulated with the Yasso20 model - which does not account for physico-chemical soil properties - and measured SOC stocks showed the largest deviations in soils with high content of stabilizing minerals

335

(Fig. 3, Fig. [S3S5](#)). The importance of different cations in stabilizing SOC depended on soil pH – confirmed by the significant interaction between pH and Ca (*P* < 0.001, Table S2, Fig. [S2S4b](#)) – which agrees with process-based studies (Rowley et al., 2018). In forest soils with pH ≤ 5, exchangeable Fe had a significant positive effect on SOC stocks (Table 2) and was the strongest predictor of SOC stocks in regions with acidic conditions (Table S5), with Yasso20 underestimating SOC stocks at high exchangeable Fe contents (Table 3, Fig. [S3S5b](#)). In soils with pH > 5, high exchangeable Ca was associated with underestimates of SOC stocks by Yasso20 (Table 3, Fig. [S3S5d](#)). Clay content - regarded as a key property for SOM stabilization (Rasmussen et al., 2018) - appeared weakly associated with SOC stocks in Swiss forest soils (Table 2, Figure 4e), which is most likely due to the overarching effect of Fe (and Al) driving the high SOC stocks in acidic, sandy

340

soils under high MAP (Table 1). Although clay normally regulates the SOC storage because of the stabilizing effect of clays on organic compounds (Alvarez and Lavado, 1998; Wiesmeier et al., 2019), we found a positive effect of clay on SOC stocks only in the Plateau region (Table S5). The negative interaction between MAP and clay content ( $P < 0.001$ , Table S2, Fig. S2a, S4a) was likely driven by the high SOC stocks in the Southern Alps, with high MAP, acidic conditions, and sandy soils (Solly et al., 2020).

Due to the low solubility product of Fe-oxides, Fe extracted with  $\text{NH}_4\text{Cl}$  comprises  $\text{Fe}^{2+}$  and/or organically bound, colloidal Fe(III)-cations (Schwertmann et al., 1987). Exchangeable Fe may, however, serve as an indicator for the content of Fe-oxides as indicated by significant correlations of  $\text{NH}_4\text{Cl}$ -extractable Fe with organically-bound Fe (pyrophosphate-extractable,  $r = +0.78$ ,  $P < 0.001$ ,  $n = 62$ ) and poorly-crystalline Fe-oxides (oxalate-extractable,  $r = +0.62$ ,  $P < 0.001$ ,  $n = 123$ ) for a subset of surface soils where Fe-oxides have been measured (Fig. S4S6). Deviations between modelled and measured SOC stocks were also related to exchangeable Al under acidic conditions (Fig. S3S5c). Since exchangeable Al was strongly correlated to exchangeable Fe ( $r = +0.87$ ), effect of Al on model deviations could not be disentangled from that of Fe and was thus excluded from the full statistical model. The dominant role of pedogenic oxides for SOM stabilization arises from their large and highly reactive mineral surfaces and positive charge under acidic and neutral conditions (Kaiser and Guggenberger, 2003), which allows interactions with SOM through cation bridging, electrostatic interactions or the formation of inner- and outer-sphere complexes (Kleber et al., 2015; Rasmussen et al., 2018). Beyond its relation to pedogenic oxides, exchangeable Fe and Al – more often available for large data sets – may represent a proxy for the weathering status of soils (Eimil-Fraga et al., 2015), which is crucial for providing reactive surfaces stabilizing SOM.

In calcareous soils, Ca-mediated SOM stabilization is linked to the ability of  $\text{Ca}^{2+}$  to bridge negatively charged organic matter surfaces when pH is above neutrality, through inner- and outer-sphere interactions and Ca-mediated aggregation (Rowley et al., 2018), which limit the decomposer activity and thus lead to preferential stabilization of organic compounds (Gocke et al., 2011; Rowley et al., 2021). However, exchangeable Ca is (similarly to exchangeable Fe for pedogenic oxides) only an indirect measure for  $\text{CaCO}_3$ . In our dataset, there was a highly significant correlation between exchangeable and  $\text{HNO}_3$ -extractable Ca for a subset of soils (0-30 cm depth,  $r = +0.60$ ,  $P < 0.001$ ,  $n = 181$ ; Fig. S5S7) and exchangeable Ca can be considered a representative measure for the carbonate content in the soil.

The pH-dependent influence of SOM-stabilizing minerals can also explain the observed differences between simulated and measured SOC stocks at regional scale (Fig. 3a, Fig. S4S3a). The largest differences, with underestimates of SOC stocks by 7  $\text{kg C m}^{-2}$ , were found in the Southern Alps. The Southern Alps are characterized by high contents of Fe- and Al-oxides (Table 1) that are considered the main drivers of the large SOC storage in this region (Blaser et al., 1997). The high SOC stocks (Fig. 3a) can additionally be related to the black carbon accumulated in these soils due to frequent forest fires and charcoal production (Eckmeier et al., 2010). Here, we could not quantify fire-derived black carbon and its potential contribution to SOM stabilization. Even when the Southern Alps were excluded from the statistical analysis, exchangeable Fe was a significant predictor of SOC stocks (Table S4a), as well as of Yasso20 deviations (Table S4b), being the predictor

explaining the largest portion of SOC stocks model variance in all regions with mostly acidic soils (Table S5). This confirms the key role of pedogenic oxides for SOM stabilization at low pH conditions.

#### 4.2 Climatic influences on SOC stocks

Beyond soil parameters, precipitation was a key driver of SOC stocks, with SOC stocks increasing with increasing MAP  
380 (Table 2, Fig. 4f). This pattern likely resulted from a number of mechanisms: (i) a retarded decomposition at anaerobic microsites (Keiluweit et al., 2017), (ii) a reduced litter quality by an increasing contribution of conifers towards higher MAP, which also coincides with low MAT at high altitudes, as confirmed by a negative correlation of MAP with MAT for elevation  $> 1000$  m ( $r = -0.43, P < 0.001$ ) that is typical for alpine regions (Prietzel and Christopel, 2014), (iii) a higher transfer of dissolved organic matter into the mineral soil with increasing soil water fluxes, and (iv) an enhanced weathering  
385 in moister climate that fosters mineral surface reactivity (Doetterl et al., 2015). Precipitation was also a significant driver of Yasso20 deviations (Table 3, Table S4), with MAP accounting for up to 20-25% of SOC stocks variance in the Alps and Plateau (Table S5). Yasso20 underestimated SOC stocks when MAP exceeded 1400 mm yr<sup>-1</sup> (Fig. S3S5f). Consistently, Viskari et al. (2022) reported that Yasso20 underestimated SOC amounts at higher precipitation, given that increasing precipitation over a certain threshold does not reduce the SOC decomposition rates in Yasso20. Current Earth System  
390 Models also tend to overestimate heterotrophic respiration fluxes where precipitation levels are high (Guenet et al., 2024). Our analysis of Yasso20 deviations, showing that SOC stocks were underestimated in waterlogged soils with macroscopic signs of anaerobic conditions (Fig. 3a), confirms that anaerobic conditions at the microscale or the impeded drainage at the profile or plot scale lead to a drastic decline in SOC mineralization rates (Hagedorn et al., 2000; Keiluweit et al., 2017). These conditions are not captured by the Yasso20 model, as soil moisture is currently not included as a model driver (Viskari  
395 et al., 2022), but could potentially be resolved in the future by including soil moisture at monthly time steps as model driver, or by applying a moisture modifier as in a boreal forest–mire ecotone in Finland for Yasso07 (Tupek et al., 2024), and/or by coupling Yasso to a soil water model (Guenet et al., 2024). Large differences between simulated and measured SOC stocks were also found in poorly drained soils of Norway and Finland using the previous version Yasso07, with soil moisture regimes overruling the importance of tree productivity (Dalsgaard et al., 2016). The model deviations were additionally  
400 attributed to the high contribution of understory vegetation in high rainfall areas (De Wit et al., 2006; Lehtonen et al., 2016). Understory including herb and shrub layers is normally not accounted in forest inventories or satellite-based NPP data (Mao et al., 2019), though it can contribute significantly to the annual litter production (Didion, 2020). In addition to its effect on the biological activity of the plant-soil system, precipitation is linked to mineral weathering, forming reactive mineral surfaces (Kramer and Chadwick, 2018). In Swiss forest soils, MAP was indeed in the same principal component (PC3) as  
405 clay (Table S1a), positively correlating with clay ( $r = +0.21, P < 0.001$ ) as well as with exchangeable Fe and Al (with Fe:  $r = +0.10, P = 0.019$ , with Al:  $r = +0.14, P < 0.001$ ) which supports the idea that high MAP may indirectly influence SOC stabilization through its effects on the reactivity of mineral surfaces. At the other extreme, at low precipitations, Lehtonen et al. (2016) observed an underestimation of SOC stocks by Yasso07, which was attributed to the poor representation of

drought effects on SOM decomposition. In fact, Yasso07 (but also Yasso20) simulations are based on yearly time steps using  
410 annual precipitation, which does not capture seasonally extreme dry or moist conditions (Lehtonen et al., 2016; Viskari et al.,  
2022) and the uneven distribution of summer precipitations (Thürig et al., 2005) thereby yielding to misestimates of soil C  
stocks.

Across Swiss forests, organic layer C stocks increased with the contribution of conifers (Table S6), likely due to a  
slower decomposition of the more recalcitrant litter inputs (Heim and Frey, 2004) and fostered by the colder conditions at  
415 higher elevations where conifers are more abundant. In our study, MAT did not significantly influence organic layer as well  
as total SOC stocks (Table 2, Table S6), possibly due to the positive correlation of MAT with the share of broadleaves ( $r =$   
+0.58,  $P < 0.001$ ) which did not allow to fully disentangle the specific effects of forest types and MAT. Accounting for the  
regional variability in the linear mixed-effect model, an overall negative effect of MAT was estimated for Yasso20  
deviations (Table 3). This finding is in agreement with the tendency of Yasso20 to underestimate SOC with increasing  
420 temperatures (Viskari et al., 2022). The Yasso model generally captures well the effects of temperature and vegetation type,  
as shown across regional environmental gradients in Swiss forests (Didion et al., 2014). Since Yasso20 deviations slightly  
increased with temperature (Fig. S3S5g) with Yasso20 overestimating SOC stocks in low-elevation broadleaf forests of the  
Swiss Plateau but not in coniferous stands at higher elevation (Fig. 3b, Fig. S1S3c), we interpret this overestimation as an  
indication for an impact of past land-use and current land management. The Plateau has intensively been used for agriculture  
425 since Roman times (Haas et al., 2020), which depleted soils in SOC (Thürig et al., 2005). It is still Switzerland's most  
intensively managed region, with harvesting exceeding tree growth increments (Thürig et al., 2021). This intensive  
management, particularly harvesting, may not be adequately captured by Yasso20 simulations. Similarly, simulations with  
Yasso07 in French temperate forests tended to overestimate SOC stocks in broadleaf stands while underestimating them in  
coniferous ones, which was attributed to historical differences in land use and stand age between broadleaf and coniferous  
430 sites (Mao et al., 2019). Here, on the one hand, harvesting depletes soil C stocks by changing the microclimate, reducing  
the litter inputs and leading to physical soil disturbances (Mayer et al., 2024). On the other hand, timber removal or other  
small-scale forest disturbances are may be poorly detected by NPP estimates satellite driven from MODIS satellite data, as  
discussed below NPP estimates (Neumann et al., 2015; Park et al., 2021).

Consequently, our MODIS derived NPP inputs likely overestimated the actual litter inputs in forests with intensive  
435 harvesting. Similarly, simulations with Yasso07 in French temperate forests tended to overestimate SOC stocks in broadleaf  
stands while underestimating them in coniferous ones, which was attributed to historical differences in land use and stand  
age between broadleaf and coniferous sites (Mao et al., 2019). Since measurements of forest stands and soil C inputs are  
often lacking at larger scales - as in this study - the satellite-derived NPP is here used as proxy of long-term litter C input to  
the soil, consistently with SOC model applications at the regional and global scales (Abramoff et al., 2022; Pierson et al.,  
440 2022), as well as with the calibration of Yasso20 (Viskari et al., 2022). Uncertainty in litter inputs potentially contributed to  
the observed discrepancies between simulated and measured SOC stocks at the site level. The fine scale variability in litter  
inputs cannot be captured by satellite-derived NPP estimates given (1) the larger pixel size of MODIS (500 m x 500 m)

445 compared to the site scale of the soil sampling, and (2) the partitioning into tree components using average allocation factors, due to the lack of site-level data. NPP estimates from MODIS may overestimate the litter input in regions with intensive  
445 forest management as in the Plateau, since small-scale disturbances such as thinning are not well detected by satellites (Neumann et al., 2015; Park et al., 2021). Lastly, forests allocate a portion of NPP not only to fast-cycling components that are annually returned to the soil (i.e. fine roots and foliage) but also to components with slower turnover time such as stems and branches. Nevertheless, the satellite approach proves to be a reasonable proxy of the large range of forest productivity across Swiss forests, i.e. ranging from  $0.3 \text{ kg C m}^{-2} \text{ yr}^{-1}$  in the Alps to  $0.8 \text{ kg C m}^{-2} \text{ yr}^{-1}$  at the warmest sites (see Fig. S1a),  
450 which is consistent with differences in wood increments across regions as shown in the Swiss NFI (Brändli et al., 2020). Moreover, at the 18 sites of the long-term forest monitoring program LWF, the mean NPP over the period 2001-2010 estimated by MODIS satellite amounted to  $0.49 \pm 0.04 \text{ kg C m}^{-2} \text{ yr}^{-1}$  as compared to  $0.46 \pm 0.05 \text{ kg C m}^{-2} \text{ yr}^{-1}$  estimated by a terrestrial approach for the same period (Etzold et al., 2014). Terrestrial methods based on forest inventories may also produce uncertain estimates of litter inputs. These uncertainties mostly relate to (1) country-specific allometries and  
455 expansion factors used to estimate tree biomass, (2) turnover times applied to derive the annual litter inputs, and (3) failing to appropriately estimate inputs from fine roots and understory vegetation, which remain severely unconstrained despite their major contribution to forest soil C inputs (Didion, 2020; Neumann et al., 2020).

### 4.3 Performance and potential improvements of Yasso20

460 Despite the local and regional deviations between SOC stocks simulated with Yasso20 and the measured ones, our study showed that averaged across Swiss forests and thus at the national scale, Yasso20 reproduced measured SOC stocks (Fig. 3), confirming the wide applicability of Yasso20 model (Viskari et al., 2022). The Yasso model was developed for general uses on primarily forest land, including GHG reporting at national level and requires less input information (no soil data) compared to more detailed soil C models (Liski et al., 2005). Yasso is compatible with biomass data from National Forest Inventories, where soil parameters are often not measured, allowing to estimate soil C stock changes (Hernández et al.,  
465 2017). Our study indicates that implementing SOM stabilization mechanisms would improve the Yasso model and potentially also other similar soil C models such as RothC model that accounts only for clay content (Coleman and Jenkinson, 2014). However, detailed soil information controlling SOM stabilization is often missing at larger scales. We therefore suggest to further explore commonly available soil parameters, potentially by simple pedo-transfer functions (e.g. based on exchangeable Fe and Ca) capturing SOC stabilization at different pH levels. A combined approach – directly coupling Yasso with a statistical model - would allow to account for additional parameters (as mineral soil properties) that are currently not included as model drivers but are known to be important factors controlling SOC stabilization. Our study  
470 also revealed that Yasso did not capture SOC stocks (and potentially SOC stock changes) at high precipitation levels (here MAP  $> 1400 \text{ mm yr}^{-1}$ ). This hampers predictions especially under extreme or variable intra-annual precipitation patterns that will become more frequent under climate change. Obviously, linking Yasso20 to a soil water model accounting for drought

475 and waterlogging processes would have a high potential for improving estimates of SOC stocks. However, a robust modeling of waterlogging would also require spatially highly resolved soil information.

Our study does not inform on the performance of Yasso20 in estimating SOC stock changes, which is the primary application of Yasso for GHG reporting. However, it seems likely that also SOC stock changes will be affected by soil physico-chemical properties, due to the importance of organo-mineral interactions for SOC stabilization and thus long-term  
480 C sequestration (Wiesmeier et al., 2019; Bramble et al., 2023). This would be congruent with the concept of soil C saturation suggesting that effects of C inputs on soil carbon storage depend upon inherent physico-chemical limitations (Stewart et al., 2007; Six et al., 2024).

## 5. Conclusions

Our study demonstrates that soil mineral properties controlling SOM stabilization play a dominant role for SOC stocks  
485 across Swiss forest soils. The control appears to be pH dependent with Fe (and Al) having a major influence in acidic soils, while interactions with Ca are most important in soils with pH values above 5. Not accounting for these processes in a soil C model designed to estimate national scale SOC stocks and their changes - based solely on litter inputs and climate - can lead to underestimating SOC stocks in certain regions, particularly those rich in SOM stabilizing minerals. Despite its simple model structure, our results show that Yasso20 yielded on average SOC stocks comparable to measured values at 556 forest  
490 sites across Switzerland. This supports Yasso20 broad applicability for predicting forest SOC stocks at larger national scales. Including SOM stabilization and linking soil C models to soil water models has a high potential to improve the accuracy of the estimates. It remains uncertain, however, whether the model lack of representation of mineral-driven SOM stabilization or/and of varying soil moisture regimes will not only affect SOC stock estimates but also expected changes in SOC stocks - the primary application of Yasso in GHG inventories.

## 495 Code and Data availability

All data used in this study are available online through EnviDat at <https://doi.org/10.16904/envidat.443> (Guidi et al., 2024). The code can be made available upon request.

## Author contributions

FH and PN conceived and designed the study. CG and SG performed data analysis and visualization and wrote the  
500 manuscript with contributions from all co-authors. All authors contributed to the interpretation of the findings, they read and approved the submitted version.

## Competing interests

One of the (co-)authors is a member of the editorial board of Biogeosciences.

## Acknowledgements

505 This study (SNF 406840\_143025) was funded by the Swiss National Fond (SNF) within the National Research Programme  
68 (Sustainable Use of Soil as a Resource). Evaluations were based on data from the Swiss Long-term Forest Ecosystem  
Research programme LWF ([www.lwf.ch](http://www.lwf.ch)), which is part of the UNECE Co-operative Programme on Assessment and  
Monitoring of Air Pollution Effects on Forests ICP Forests ([www.icp-forests.net](http://www.icp-forests.net)). We are particularly grateful to Peter  
Waldner for the provision of the LWF data, to Oliver Schramm for the collection of the data, and to Peter Jakob for the  
510 technical support on the database. The authors also especially acknowledge Flurin Sutter for helping with preparation of Fig.  
1, Achilleas Psomas for his support with obtaining NPP data and Sophia Etzold for providing long-term tree allocation data  
in LWF. We also acknowledge Jürgen Zell and Sebastian Doetterl for fruitful discussions on statistical analysis of an earlier  
version of the manuscript.

## References

515 Abramoff, R., Xu, X., Hartman, M., O'Brien, S., Feng, W., Davidson, E., Finzi, A., Moorhead, D., Schimel, J., and Torn, M.: The Millennial model: in search of measurable pools and transformations for modeling soil carbon in the new century, *Biogeochemistry*, 137, 51-71, 2018.

Abramoff, R. Z., Guenet, B., Zhang, H., Georgiou, K., Xu, X., Rossel, R. A. V., Yuan, W., and Ciais, P.: Improved global-scale predictions of soil carbon stocks with Millennial Version 2, *Soil Biology and Biochemistry*, 164, 108466, 2022.

520 Ågren, G. I., Hyvönen, R., and Nilsson, T.: Are Swedish forest soils sinks or sources for CO<sub>2</sub>—model analyses based on forest inventory data, *Biogeochemistry*, 89, 139-149, 2008.

Alvarez, R. and Lavado, R. S.: Climate, organic matter and clay content relationships in the Pampa and Chaco soils, Argentina, *Geoderma*, 83, 127-141, 1998.

525 Angst, G., Messinger, J., Greiner, M., Häusler, W., Hertel, D., Kirfel, K., Kögel-Knabner, I., Leuschner, C., Rethemeyer, J., and Mueller, C. W.: Soil organic carbon stocks in topsoil and subsoil controlled by parent material, carbon input in the rhizosphere, and microbial-derived compounds, *Soil Biology and Biochemistry*, 122, 19-30, 2018.

Berg, B., Bootink, H., Breymeyer, A., Ewertsson, A., Gallardo, A., Holm, B., Johansson, M., Koivuoa, S., Meentemeyer, V., and Nyman, P.: Data on needle litter decomposition and soil climate as well as site characteristics for some coniferous forest sites, 2: Decomposition data, 1991.

530 Blaser, P., Kernebeek, P., Tebbens, L., Van Breemen, N., and Luster, J.: Cryptopodzolic soils in Switzerland, *European Journal of Soil Science*, 48, 411-423, 1997.

Bramble, D. S. E., Ulrich, S., Schöning, I., Mikutta, R., Brandt, L., Poll, C., Kandeler, E., Mikutta, C., Konrad, A., and Siemens, J.: Formation of mineral-associated organic matter in temperate soils is primarily controlled by mineral type and modified by land use and management intensity, *Global Change Biology*, e17024, 2023.

535 Brändli, U.-B., Abegg, M., and Allgaier, B. L.: Schweizerisches Landesforstinventar: Ergebnisse der vierten Erhebung 2009-2017, WSL2020.

Braun-Blanquet, J.: *Pflanzensoziologie. Grundzüge der Vegetationskunde*, Springer Vienna, Vienna, 865, 10.1007/978-3-7091-8110-2, 1964.

Brunmayr, A. S., Hagedorn, F., Moreno Duborgel, M., Minich, L. I., and Graven, H. D.: Radiocarbon analysis reveals 540 underestimation of soil organic carbon persistence in new-generation soil models, *Geosci. Model Dev.*, 17, 5961-5985, 10.5194/gmd-17-5961-2024, 2024.

Chen, S., Huang, Y., Zou, J., and Shi, Y.: Mean residence time of global topsoil organic carbon depends on temperature, precipitation and soil nitrogen, *Global and Planetary Change*, 100, 99-108, 2013.

545 Coleman, K. and Jenkinson, D.: RothC—A model for the turnover of carbon in soil Model—Model description and users guide, 2014.

Dalsgaard, L., Lange, H., Strand, L. T., Callesen, I., Borgen, S. K., Liski, J., and Astrup, R.: Underestimation of boreal forest soil carbon stocks related to soil classification and drainage, *Canadian Journal of Forest Research*, 46, 1413-1425, 2016.

de Wit, H. A., Palosuo, T., Hylen, G., and Liski, J.: A carbon budget of forest biomass and soils in southeast Norway calculated using a widely applicable method, *Forest Ecology and Management*, 225, 15-26, 2006.

550 Didion, M.: Extending harmonized national forest inventory herb layer vegetation cover observations to derive comprehensive biomass estimates, *Forest Ecosystems*, 7, 1-14, 2020.

Didion, M.: Data on soil carbon stock change, carbon stock and stock change in surface litter and in coarse dead wood prepared for the Swiss NIR 2024 (GHGI 1990–2022), 2023.

555 Didion, M., Frey, B., Rogiers, N., and Thürig, E.: Validating tree litter decomposition in the Yasso07 carbon model, *Ecological Modelling*, 291, 58-68, 2014.

Didion, M., Blujdea, V., Grassi, G., Hernández, L., Jandl, R., Kriiska, K., Lehtonen, A., and Saint-André, L.: Models for reporting forest litter and soil C pools in national greenhouse gas inventories: methodological considerations and requirements, *Carbon Management*, 7, 79-92, 2016.

560 Doetterl, S., Berhe, A. A., Arnold, C., Bodé, S., Fiener, P., Finke, P., Fuchslueger, L., Griepentrog, M., Harden, J., and Nadeu, E.: Links among warming, carbon and microbial dynamics mediated by soil mineral weathering, *Nature Geoscience*, 11, 589-593, 2018.

Doetterl, S., Stevens, A., Six, J., Merckx, R., Van Oost, K., Casanova Pinto, M., Casanova-Katny, A., Muñoz, C., Boudin, M., and Zagal Venegas, E.: Soil carbon storage controlled by interactions between geochemistry and climate, *Nature Geoscience*, 8, 780-783, 2015.

565 Eckmeier, E., Egli, M., Schmidt, M., Schlumpf, N., Nötzli, M., Minikus-Stary, N., and Hagedorn, F.: Preservation of fire-derived carbon compounds and sorptive stabilisation promote the accumulation of organic matter in black soils of the Southern Alps, *Geoderma*, 159, 147-155, 2010.

Eimil-Fraga, C., Álvarez-Rodríguez, E., Rodríguez-Soalleiro, R., and Fernández-Sanjurjo, M. J.: Influence of parent material on the aluminium fractions in acidic soils under *Pinus pinaster* in Galicia (NW Spain), *Geoderma*, 255, 50-57, 2015.

570 Etzold, S., Waldner, P., Thimonier, A., Schmitt, M., and Dobbertin, M.: Tree growth in Swiss forests between 1995 and 2010 in relation to climate and stand conditions: Recent disturbances matter, *Forest Ecology and Management*, 311, 41-55, 2014.

Fischer, C. and Traub, B.: Swiss National Forest Inventory - Methods and Models of the Fourth assessment. *Managing forest ecosystems*, 35 431 p., Springer, 10.1007/978-3-030-19293-8, 2019.

575 Gee, G. W. and Bauder, J. W.: Particle-size analysis, *Methods of soil analysis: Part 1 Physical and mineralogical methods*, 5, 383-411, 1986.

Gholz, H. L., Wedin, D. A., Smitherman, S. M., Harmon, M. E., and Parton, W. J.: Long-term dynamics of pine and hardwood litter in contrasting environments: toward a global model of decomposition, *Global Change Biology*, 6, 751-765, 2000.

580 Gimmi, U., Poulter, B., Wolf, A., Portner, H., Weber, P., and Bürgi, M.: Soil carbon pools in Swiss forests show legacy effects from historic forest litter raking, *Landscape Ecology*, 28, 835-846, 2013.

Gnägi, C. and Labhart, T.: *Geologie der Schweiz*, Ott Verlag. 2015.

Gocke, M., Pustovoytov, K., and Kuzyakov, Y.: Pedogenic carbonate recrystallization assessed by isotopic labeling: a comparison of <sup>13</sup>C and <sup>14</sup>C tracers, *Journal of Plant Nutrition and Soil Science*, 174, 809-817, 2011.

585 Gosheva, S., Walther, L., Niklaus, P. A., Zimmermann, S., Gimmi, U., and Hagedorn, F.: Reconstruction of historic forest cover changes indicates minor effects on carbon stocks in Swiss forest soils, *Ecosystems*, 20, 1512-1528, 2017.

Guenet, B., Orliac, J., Cécillon, L., Torres, O., Sereni, L., Martin, P. A., Barré, P., and Bopp, L.: Spatial biases reduce the ability of Earth system models to simulate soil heterotrophic respiration fluxes, *Biogeosciences*, 21, 657-669, 2024.

590 Guidi, C., Zimmermann, S., Walther, L., Didion, M., Gosheva-Oney, S., and Hagedorn, F.: Soil organic carbon drivers in the Swiss forest soil inventory, *EnviDat* <https://doi.org/10.16904/envidat.443> [dataset], 2024.

Haas, M., Kaltenrieder, P., Ladd, S. N., Welte, C., Strasser, M., Eglinton, T. I., and Dubois, N.: Land-use evolution in the catchment of Lake Murten, Switzerland, *Quaternary Science Reviews*, 230, 106154, 2020.

Hagedorn, F., Kaiser, K., Feyen, H., and Schleppi, P.: Effects of Redox Conditions and Flow Processes on the Mobility of Dissolved Organic Carbon and Nitrogen in a Forest Soil, *Journal of Environmental Quality*, 29, 288-297, 595 <https://doi.org/10.2134/jeq2000.00472425002900010036x>, 2000.

Hagedorn, F., Moeri, A., Walther, L., and Zimmermann, S.: Kohlenstoff in Schweizer Waldböden—bei Klimaerwärmung eine potenzielle CO<sub>2</sub>-Quelle| Soil organic carbon in Swiss forest soils—a potential CO<sub>2</sub> source in a warming climate, Schweizerische Zeitschrift für Forstwesen, 161, 530-535, 2010.

600 Hagedorn, F., Spinnler, D., Bundt, M., Blaser, P., and Siegwolf, R.: The input and fate of new C in two forest soils under elevated CO<sub>2</sub>, Global Change Biology, 9, 862-872, 2003.

Heim, A. and Frey, B.: Early stage litter decomposition rates for Swiss forests, Biogeochemistry, 70, 299-313, 2004.

Hernández, L., Jandl, R., Blujdea, V. N., Lehtonen, A., Kriiska, K., Alberdi, I., Adermann, V., Cañellas, I., Marin, G., and Moreno-Fernández, D.: Towards complete and harmonized assessment of soil carbon stocks and balance in forests: The ability of the Yasso07 model across a wide gradient of climatic and forest conditions in Europe, Science of The Total Environment, 599, 1171-1180, 2017.

605 IUSS: Working Group WRB. World Reference Base for Soil Resources 2006, first update 2007, FAO, Rome, 1-128 pp.2007.

Kaiser, K. and Guggenberger, G.: Mineral surfaces and soil organic matter, European Journal of Soil Science, 54, 219-236, 2003.

610 Keiluweit, M., Wanzek, T., Kleber, M., Nico, P., and Fendorf, S.: Anaerobic microsites have an unaccounted role in soil carbon stabilization, Nature communications, 8, 1771, 2017.

Kleber, M., Eusterhues, K., Keiluweit, M., Mikutta, C., Mikutta, R., and Nico, P. S.: Mineral–organic associations: formation, properties, and relevance in soil environments, Advances in agronomy, 130, 1-140, 2015.

615 Kramer, M. G. and Chadwick, O. A.: Climate-driven thresholds in reactive mineral retention of soil carbon at the global scale, Nature Climate Change, 8, 1104-1108, 2018.

Lehmann, J. and Kleber, M.: The contentious nature of soil organic matter, Nature, 528, 60-68, 2015.

Lehtonen, A., Linkosalo, T., Peltoniemi, M., Sievänen, R., Mäkipää, R., Tamminen, P., Salemaa, M., Nieminen, T., Tupek, B., and Heikkinen, J.: Forest soil carbon stock estimates in a nationwide inventory: evaluating performance of the ROMULv and Yasso07 models in Finland, Geoscientific Model Development, 9, 4169-4183, 2016.

620 Liski, J., Palosuo, T., Peltoniemi, M., and Sievänen, R.: Carbon and decomposition model Yasso for forest soils, Ecological modelling, 189, 168-182, 2005.

Lüdecke, D., Ben-Shachar, M. S., Patil, I., Waggoner, P., and Makowski, D.: performance: An R package for assessment, comparison and testing of statistical models, Journal of Open Source Software, 6, 2021.

625 Luo, Z., Viscarra-Rossel, R. A., and Qian, T.: Similar importance of edaphic and climatic factors for controlling soil organic carbon stocks of the world, *Biogeosciences*, 18, 2063-2073, 2021.

Mäkinen, H., Hynynen, J., Saitonen, J., and Sievänen, R.: Predicting the decomposition of Scots pine, Norway spruce, and birch stems in Finland, *Ecological Applications*, 16, 1865-1879, 2006.

630 Mao, Z., Derrien, D., Didion, M., Liski, J., Eglin, T., Nicolas, M., Jonard, M., and Saint-André, L.: Modeling soil organic carbon dynamics in temperate forests with Yasso07, *Biogeosciences*, 16, 1955-1973, 2019.

Mayer, M., Baltensweiler, A., James, J., Rigling, A., and Hagedorn, F.: A global synthesis and conceptualization of the magnitude and duration of soil carbon losses in response to forest disturbances, *Global Ecology and Biogeography*, 33, 141-150, 2024.

635 Mayer, M., Rusch, S., Didion, M., Baltensweiler, A., Walthert, L., Ranft, F., Rigling, A., Zimmermann, S., and Hagedorn, F.: Elevation dependent response of soil organic carbon stocks to forest windthrow, *Science of the Total Environment*, 857, 159694, 2023.

Mayer, M., Prescott, C. E., Abaker, W. E., Augusto, L., Cécillon, L., Ferreira, G. W., James, J., Jandl, R., Katzensteiner, K., and Laclau, J.-P.: Tamm Review: Influence of forest management activities on soil organic carbon stocks: A knowledge synthesis, *Forest Ecology and Management*, 466, 118127, 2020.

640 MeteoSwiss: Federal Office of Meteorology and Climatology. Spatial Climate Analyses. <https://www.meteoswiss.admin.ch/home/climate/swiss-climate-in-detail/raeumliche-klimaanalysen.html>. Accessed 19.01.2024, 2024.

Neumann, M., Godbold, D. L., Hirano, Y., and Finér, L.: Improving models of fine root carbon stocks and fluxes in European forests, *Journal of Ecology*, 108, 496-514, 2020.

645 Neumann, M., Zhao, M., Kindermann, G., and Hasenauer, H.: Comparing MODIS net primary production estimates with terrestrial national forest inventory data in Austria, *Remote Sensing*, 7, 3878-3906, 2015.

Nussbaum, M., Papritz, A., Zimmermann, S., and Walthert, L.: Pedotransfer function to predict density of forest soils in Switzerland, *Journal of Plant Nutrition and Soil Science*, 179, 321-326, 2016.

Park, J. H., Gan, J., and Park, C.: Discrepancies between global forest net primary productivity estimates derived from MODIS and forest inventory data and underlying factors, *Remote Sensing*, 13, 1441, 2021.

650 Pierson, D., Lohse, K. A., Wieder, W. R., Patton, N. R., Facer, J., de Graaff, M.-A., Georgiou, K., Seyfried, M. S., Flerchinger, G., and Will, R.: Optimizing process-based models to predict current and future soil organic carbon stocks at high-resolution, *Scientific Reports*, 12, 10824, 2022.

Pinheiro, J., Bates, D., and R Core Team: nlme: Linear and Nonlinear Mixed Effects Models. R package version 3.1-160, <https://CRAN.R-project.org/package=nlme>., 2022.

655 Prescott, C. E. and Grayston, S. J.: TAMM review: Continuous root forestry—Living roots sustain the belowground ecosystem and soil carbon in managed forests, *Forest Ecology and Management*, 532, 120848, 2023.

Prietzl, J. and Christophel, D.: Organic carbon stocks in forest soils of the German Alps, *Geoderma*, 221, 28-39, 2014.

Prietzl, J., Zimmermann, L., Schubert, A., and Christophel, D.: Organic matter losses in German Alps forest soils since the 1970s most likely caused by warming, *Nature Geoscience*, 9, 543-548, 2016.

660 Pusa, J.: Ryassofortran: Provides functionality for calling the YASSO15 Fortran-release in R. R package version 0.4.0. <https://github.com/YASSOmodel/Ryassofortran>, 2023.

R Core Team: R: A language and environment for statistical computing. R Foundation for Statistical Computing, Vienna, Austria. <https://www.R-project.org/>. 2022.

Rasmussen, C., Heckman, K., Wieder, W. R., Keiluweit, M., Lawrence, C. R., Berhe, A. A., Blankinship, J. C., Crow, S. E.,  
665 Druhan, J. L., and Hicks Pries, C. E.: Beyond clay: towards an improved set of variables for predicting soil organic matter content, *Biogeochemistry*, 137, 297-306, 2018.

Reichenbach, M., Fiener, P., Hoyt, A., Trumbore, S., Six, J., and Doetterl, S.: Soil carbon stocks in stable tropical landforms are dominated by geochemical controls and not by land use, *Global Change Biology*, 29, 2591-2607, 2023.

Richard, F., Lüscher, P., and Strobel, T.: Physikalische Eigenschaften von Böden der Schweiz, Eidgenössischen Anstalt für  
670 das forstliche Versuchswesen 1978.

Rowley, M. C., Grand, S., and Verrecchia, É. P.: Calcium-mediated stabilisation of soil organic carbon, *Biogeochemistry*, 137, 27-49, 2018.

Rowley, M. C., Grand, S., Spangenberg, J. E., and Verrecchia, É. P.: Evidence linking calcium to increased organo-mineral association in soils, *Biogeochemistry*, 153, 223-241, 2021.

675 Running, S. and Zhao, M.: MODIS/Aqua Net Primary Production Gap-Filled Yearly L4 Global 500m SIN Grid V061. Distributed by NASA EOSDIS Land Processes Distributed Active Archive Center. <https://doi.org/10.5067/MODIS/MYD17A3HGF.061>. Accessed 2024-01-03., 2021a.

Running, S. and Zhao, M.: MODIS/Terra Net Primary Production Gap-Filled Yearly L4 Global 500m SIN Grid V061. Distributed by NASA EOSDIS Land Processes Distributed Active Archive Center,  
680 <https://doi.org/10.5067/MODIS/MOD17A3HGF.061>. Accessed 2024-01-03, 2021b.

Schmidt, M. W., Torn, M. S., Abiven, S., Dittmar, T., Guggenberger, G., Janssens, I. A., Kleber, M., Kögel-Knabner, I., Lehmann, J., and Manning, D. A.: Persistence of soil organic matter as an ecosystem property, *Nature*, 478, 49-56, 2011.

Schrumpf, M., Schulze, E., Kaiser, K., and Schumacher, J.: How accurately can soil organic carbon stocks and stock changes be quantified by soil inventories?, *Biogeosciences*, 8, 1193-1212, 2011.

685 Schwertmann, U., Süsser, P., and Nätscher, L.: Protonenpuffersubstanzen in Böden, *Zeitschrift für Pflanzenernährung und Bodenkunde*, 150, 174-178, 1987.

Sierra, C. A., Müller, M., Metzler, H., Manzoni, S., and Trumbore, S. E.: The muddle of ages, turnover, transit, and residence times in the carbon cycle, *Global Change Biology*, 23, 1763-1773, 2017.

690 Six, J., Doetterl, S., Laub, M., Müller, C. R., and Van de Broek, M.: The six rights of how and when to test for soil C saturation, *SOIL*, 10, 275-279, 2024.

Smith, P., Soussana, J. F., Angers, D., Schipper, L., Chenu, C., Rasse, D. P., Batjes, N. H., Van Egmond, F., McNeill, S., and Kuhnert, M.: How to measure, report and verify soil carbon change to realize the potential of soil carbon sequestration for atmospheric greenhouse gas removal, *Global Change Biology*, 26, 219-241, 2020.

695 Solly, E. F., Weber, V., Zimmermann, S., Walther, L., Hagedorn, F., and Schmidt, M. W.: A critical evaluation of the relationship between the effective cation exchange capacity and soil organic carbon content in Swiss forest soils, *Frontiers in Forests and Global Change*, 3, 98, 2020.

Stewart, C. E., Paustian, K., Conant, R. T., Plante, A. F., and Six, J.: Soil carbon saturation: concept, evidence and evaluation, *Biogeochemistry*, 86, 19-31, 2007.

Swisstopo: DEM. <https://www.swisstopo.admin.ch/de/home.html> Swiss Federal Office of Topography, 2011.

700 Thürig, E., Stadelmann, G., and Didion, M.: Estimating carbon stock changes in living and dead biomass and soil for the technical correction of Switzerland's Forest Management Reference Level for the Swiss NIR 2021 (1990–2019) – modeling methodology and results. *Forest Resources and Management*, Swiss Federal Institute for Forest, Snow and Landscape Research WSL, 2021.

Thürig, E., Palosuo, T., Bucher, J., and Kaufmann, E.: The impact of windthrow on carbon sequestration in Switzerland: a 705 model-based assessment, *Forest Ecology and Management*, 210, 337-350, 2005.

Trofymow, J. A.: The Canadian Intersite Decomposition Experiment (CIDET): project and site establishment report, BC-X-3781998.

Tuomi, M., Thum, T., Järvinen, H., Fronzek, S., Berg, B., Harmon, M., Trofymow, J., Sevanto, S., and Liski, J.: Leaf litter decomposition—Estimates of global variability based on Yasso07 model, *Ecological Modelling*, 220, 3362-3371, 2009.

710 Tupek, B., Lehtonen, A., Yurova, A., Abramoff, R., Guenet, B., Bruni, E., Launiainen, S., Peltoniemi, M., Hashimoto, S., and Tian, X.: Modelling boreal forest's mineral soil and peat C dynamics with the Yasso07 model coupled with the Ricker moisture modifier, *Geoscientific Model Development*, 17, 5349-5367, 2024.

van der Voort, T. S., Zell, C., Hagedorn, F., Feng, X., McIntyre, C., Haghipour, N., Graf Pannatier, E., and Eglinton, T. I.: Diverse soil carbon dynamics expressed at the molecular level, *Geophysical Research Letters*, 44, 11,840-811,850, 2017.

715 Vesterdal, L., Clarke, N., Sigurdsson, B. D., and Gundersen, P.: Do tree species influence soil carbon stocks in temperate and boreal forests?, *Forest Ecology and Management*, 309, 4-18, 2013.

Viskari, T., Pusa, J., Fer, I., Repo, A., Vira, J., and Liski, J.: Calibrating the soil organic carbon model Yasso20 with multiple datasets, *Geoscientific Model Development*, 15, 1735-1752, 2022.

720 Walthert, L., Pannatier, E. G., and Meier, E. S.: Shortage of nutrients and excess of toxic elements in soils limit the distribution of soil-sensitive tree species in temperate forests, *Forest ecology and management*, 297, 94-107, 2013.

Walthert, L., Zimmermann, S., Blaser, P., Luster, J., and Lüscher, P.: Waldböden der Schweiz. Band 1. Grundlagen und Region Jura.(Forest soils of Switzerland. Vol. 1. Basics and the Jura Region), 2004.

725 Walthert, L., Graf, U., Kammer, A., Luster, J., Pezzotta, D., Zimmermann, S., and Hagedorn, F.: Determination of organic and inorganic carbon,  $\delta^{13}\text{C}$ , and nitrogen in soils containing carbonates after acid fumigation with HCl, *Journal of Plant Nutrition and Soil Science*, 173, 207-216, 2010.

Wiesmeier, M., Prietzel, J., Barthold, F., Spörlein, P., Geuß, U., Hangen, E., Reischl, A., Schilling, B., von Lützow, M., and Kögel-Knabner, I.: Storage and drivers of organic carbon in forest soils of southeast Germany (Bavaria)—Implications for carbon sequestration, *Forest ecology and management*, 295, 162-172, 2013.

730 Wiesmeier, M., Urbanski, L., Hobley, E., Lang, B., von Lützow, M., Marin-Spiotta, E., van Wesemael, B., Rabot, E., Ließ, M., and Garcia-Franco, N.: Soil organic carbon storage as a key function of soils-A review of drivers and indicators at various scales, *Geoderma*, 333, 149-162, 2019.

Zinke, P. J., Millemann, R. E., and Boden, T. A.: Worldwide organic soil carbon and nitrogen data, *Carbon Dioxide Information Center, Environmental Sciences Division*. 1986.